Available online at www.sciencedirect.com
SCIENCE DIRECT®
ELSEVIER
Applied Numerical Mathematics 55 (2005) 458–472
APPLIED NUMERICAL MATHEMATICS
www.elsevier.com/locate/apnum

Non-degeneracy study of the 8-tetrahedra longest-edge partition

Angel Plaza [a,*], Miguel A. Padrón [b], José P. Suárez [c]

[a] *Department of Mathematics, University of Las Palmas de Gran Canaria, 35017 Las Palmas de Gran Canaria, Spain*
[b] *Department of Civil Engineering, ULPGC, 35017 Las Palmas de Gran Canaria, Spain*
[c] *Department of Graphic Engineering, ULPGC, 35017 Las Palmas de Gran Canaria, Spain*

Available online 26 January 2005

Abstract

In this paper we show empirical evidence on the non-degeneracy property of the tetrahedral meshes obtained by iterative application of the 8-tetrahedra longest-edge (8T-LE) partition. The 8T-LE partition of an initial tetrahedron t yields an infinite sequence of tetrahedral meshes $\tau^1 = \{t\},\ \tau^2 = \{t_i^2\},\ \tau^3 = \{t_i^3\}, \ldots$. We give numerical experiments showing that for a standard shape measure introduced by Liu and Joe (η), the non-degeneracy convergence to a fixed positive value is guaranteed, that is, for any tetrahedron t_i^n in τ^n, $n \geqslant 1$, $\eta(t_i^n) \geqslant c\eta(t)$ where c is a positive constant independent of i and n. Based on our experiments, estimates of c are provided.

Keywords: Mesh quality; Degeneracy; 8-tetrahedra longest-edge partition

1. Introduction

Unstructured mesh generation and adaptive mesh refinement methods for two- and three-dimensional complex domains are very successful tools for the efficient solution of numerical application problems. A major drawback of these methods is that they may produce poorly shaped elements causing the numerical solution to be less accurate and more difficult to compute [1,19].

In [14] Rivara and Levin considered a pure three-dimensional longest-edge refinement method. Empirical experimentation was provided showing that the solid angle decreases slowly with the refinement iteration, and that a quality-element improvement behavior, holds in practice, as in the two-dimensional

* Corresponding author.
E-mail address: aplaza@dmat.ulpgc.es (A. Plaza).

0168-9274/$30.00
doi:10.1016/j.apnum.2004.12.003

case. However, there have not been mathematical results guaranteeing the non-degeneracy property of the 3-dimensional mesh.

In this paper, we focus on the non-degeneracy property of 8-tetrahedra longest-edge (8T-LE) partition, which is the natural extension to three dimensions of the well-known 4-triangles longest-edge partition introduced by Rivara [12]. The non-degeneracy property has been observed for the 8T-LE partition and also for the associated local refinement, the 3D-SBR (3D skeleton based refinement) algorithm introduced by Plaza and Carey [9].

We design a number of experiments that allow us to state the conjecture that the non-degeneracy property of the 8T-LE partition holds in 3D. Furthermore, the behavior of the non-degeneracy in the 8T-LE partition is similar to that of other partitions used in the literature [4,14].

The paper is organized as follows: Several definitions of partitioning in two and three dimensions are given in Section 2. The 8-tetrahedra longest-edge partition is explained in Section 3. Section 4 presents measures of the quality of the simplices from which the Liu–Joe η measure will be selected, and some first comparison among edge bisection partition in 3D is given. The experimental part of the paper, the main one, starts in Section 5 with the introduction of the sensitivity techniques that we use for the experiments carried out in Section 6.

2. Definitions and preliminaries

A major class of refinement methods is based on the simplex bisection. Two of the most used bisection-based partitions in two dimensions are the pure longest-edge bisection and the 4-triangle longest-edge bisection. The 4-*triangles longest-edge* (4T-LE) partition has been introduced and studied by Rivara and co-authors for the last 15 years [12–15].

Definition 1 (*LE bisection and* 4*T-LE partition*). The longest-edge (LE) partition of a triangle t_1 is obtained by joining the midpoint of the longest edge of t_1 with the opposite vertex (Fig. 1(a)).

The 4T-LE partition is obtained by joining the midpoint of the longest edge with the opposite vertex and with the midpoints of the two remaining edges (see Fig. 1(b)).

Another bisection is the *newest vertex bisection* presented by Mitchell [7].

Definition 2 (*newest vertex bisection*). The newest vertex bisection of a triangle t is obtained by connecting one of the vertices, called *peak*, to the midpoint of the opposite edge, called the *base*, as in Fig. 2.

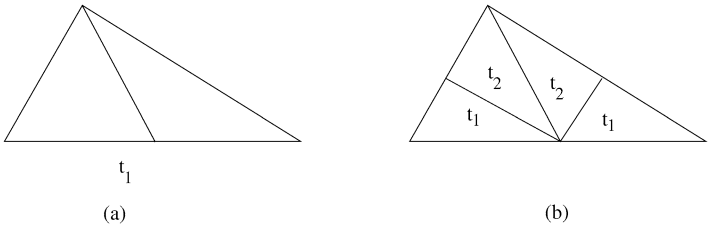

Fig. 1. (a) LE partition of triangle t_1; (b) 4T-LE partition of triangle t_1.

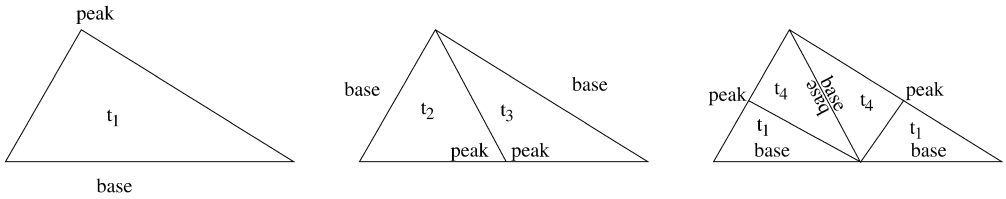

Fig. 2. Newest vertex bisection and propagation of the peak.

The peak is usually chosen to be the opposite vertex to the longest edge. Note that once the peak (or the base which is always the opposite edge to the peak) has been selected in the initial triangle, the partition works in all the successors without any computation. It is easily shown that only four similarity classes of triangles and only eight distinct angles are created by this method, so the angles satisfy the important condition of being bounded away from 0 and π. As noted by Babuška and Aziz [1] when the maximum angle approaches π, the interpolation error grows.

Based on [16] it has been proved that the longest-edge bisection, the 4T-LE partition, and in some cases also the Mitchell partition, verify the following well-known property of non-degeneracy [7,12]:

Theorem 3. *The iterative use of the Mitchell partition if the peak is chosen to be the opposite vertex to the longest edge, the longest-edge bisection, and the 4T-LE partition, applied over any initial triangulation, only produce triangles whose smallest interior angles are always greater than or equal to* $\frac{\alpha}{2}$*, where* α *is the smallest interior angle of the initial triangulation.*

Note that implementing the LE and 4T-LE partitions require the computation of the lengths. Also, very often the 4T-LE partition of a triangle and its successors is equivalent to two successive steps of the Mitchell partition [7]. However, and contrary to the Mitchell partition, the application of the 4T-LE partition shows the following self-improvement property [12,15]:

Theorem 4. *For any obtuse triangle* t_0 *of smallest angle* α_0 *and largest angle* γ_0*, the 4T-LE partition of* t_0 *produces a unique similarly distinct triangle* t_1*, whose 4T-LE partition in turn produces a new similarly distinct triangle* t_2*, and so on, until a last non-obtuse triangle* t_n *is obtained. Furthermore, the smallest angles* α_i *and the largest angles* γ_i *of triangles* t_i *satisfy the following improvement relations*: $\alpha_0 < \alpha_1 < \cdots < \alpha_n$; $\gamma_0 > \gamma_1 > \cdots > \gamma_n$.

Several techniques have been developed in three dimensions in recent years for refining (and coarsening) tetrahedral meshes by means of bisection.

Definition 5 (3*D longest-edge* (*LE*) *bisection*). The longest-edge (LE) partition of a tetrahedron t is obtained by joining the midpoint of the longest edge of t with the opposite edge.

One of the approaches based on bisection is that of Liu and Joe [4,6]. This partition can be understood as the 3D version of the Mitchell partition. The edges for bisection are chosen without any computation following a rule between the edge types involved and their relative position [4,6] to automatically assign the types to the new edges.

The partition can also be explained by means of a mapping between the original tetrahedron T and a canonical tetrahedron P with the same volume as T [6]:

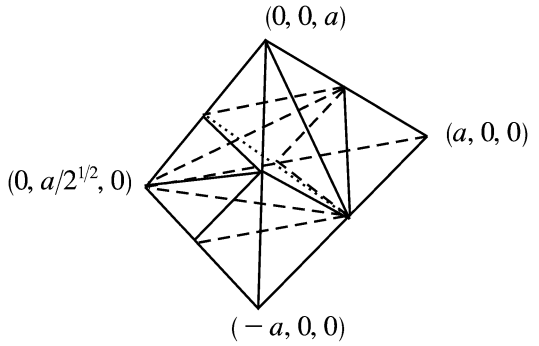

Fig. 3. Canonical Liu–Joe tetrahedron.

Definition 6 (*Liu–Joe partition*). Let T be any tetrahedron and let P be the special tetrahedron of Fig. 3 with the same volume as T. Then

(a) Transform T to P by the affine transformation $y = M^{-1}(P, T)x + b_0$.
(b) Iteratively bisect P to three levels, always bisecting the longest-edge.
(c) Transform the 8 sub-tetrahedra P_i of P back to sub-tetrahedra T_i of T using the inverse affine transformation $y = M(P, T)x + b_1$.

Fig. 3 shows the partition in eight tetrahedra of the canonical Liu–Joe tetrahedron. This tetrahedron has the interesting property that its partition in 8 sub-tetrahedra yields 8 tetrahedra similar to the former one.

Since in the sub-tetrahedra of T the longest-edge may not be the one that is bisected, this partition is not equivalent to three levels of the longest-edge partition.

Theorem 7. *Let t_1 be an initial tetrahedron. The application of the Liu–Joe partition to t_1 and all its successors yields a sequence of tetrahedral meshes $\tau^1, \tau^2, \tau^3, \ldots$. Then, for any tetrahedron t_i^n in τ^n a positive constant c exists such that, $\eta(t_i^n) \geqslant c\eta(t_1)$, where c is independent of t_1 and n.*

Moreover, it has been mathematically proved that $c \geqslant 0.1417$ [4], although numerical experiments suggest that a better estimates of c can be given.

Lastly, a partition in eight tetrahedra based on the length of the edges, the 8-tetrahedra longest-edge partition, has been investigated and used for refining and coarsening tetrahedral meshes [9,10].

3. The 8-tetrahedra longest-edge partition

Definition 8 (8-*tetrahedra longest-edge* (8*T-LE*) *partition*). For any tetrahedron t, the 8T-LE of t produces 8 sub-tetrahedra by performing the 4T-LE partition of the faces of t, and by subdividing the interior of the tetrahedron t consistently with the division of the faces (see Figs. 1 and 4).

The 8T-LE partition can be achieved by performing a sequence of bisections by the midpoints of the edges of the original tetrahedron taking into account the length of the edges as follows [11]:

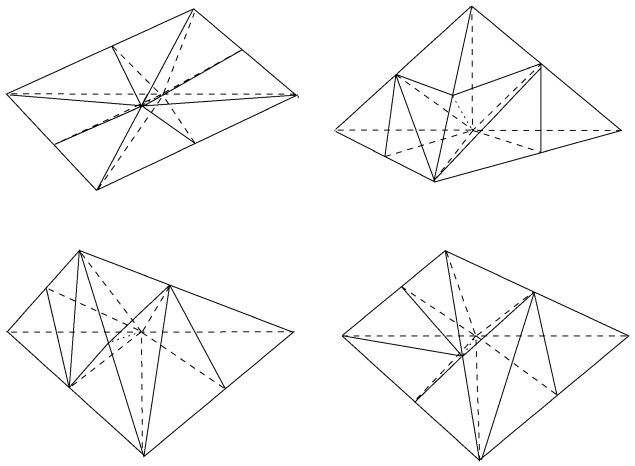

Fig. 4. Refinement patterns for the 8T-LE partition.

Theorem 9. *For any tetrahedron t of unique longest-edge, the 8T-LE partition of t is obtained as follows*:

(1) *Longest edge bisection of t producing tetrahedra t_1, t_2.*
(2) *Bisection of t_i, for $i = 1, 2$, by the longest edge of the common face of t_i with the original tetrahedron t, producing tetrahedra t_{ij}, for $j = 1, 2$.*
(3) *Bisection of each t_{ij} by the midpoint of the unique edge equal to an edge of the original tetrahedron.*

Fig. 4 shows the four refinement patterns given by the relative positions of the longest edges of the faces of the tetrahedron. Note that the 8T-LE partition is the extension to 3 dimensions of the 4T-LE partition, in the sense that this partition takes into account the longest-edge of the tetrahedra and their faces.

To conclude this section, we illustrate the practical use of the local refinement based on the 8T-LE partition to solve (adaptively) the Poisson equation with Dirichlet boundary conditions over a cube domain:

$$\begin{aligned} -\Delta u &= f \quad \text{in } \Omega, \\ u &= 0 \quad \text{in } \partial\Omega, \end{aligned} \tag{1}$$

where $\Omega = [0,1]^3$ is the unit cube. Function f is chosen in such a way that $u_{ex} = (x^2 - x)(y^2 - y)(z^2 - z)e^{-\alpha[(x-a)^2+(y-b)^2+(z-c)^2]}$ is the exact solution of the problem. Note that function $u_{ex} \in C^\infty(\Omega)$, but it has a high gradient near the point (a, b, c) for high values of α. We have chosen $\alpha = 100$ and $(a, b, c) = (0.25, 0.25, 0.25)$. The tetrahedralization of Fig. 5 was adaptively constructed to solve problem (1) starting with a 5-tetrahedra initial triangulation of the cube. Fig. 5 shows the trace on the cube surface (a) and the complete final mesh (b).

4. Shape measures and longest-edge quality measure comparison

We refer to the papers of Liu and Joe [4–6], for the definitions, discussions and equations of different tetrahedron shape measures. Other reviews of tetrahedron shape measures appear in Dompierre et al. [3] and Parthasarathy et al. [8].

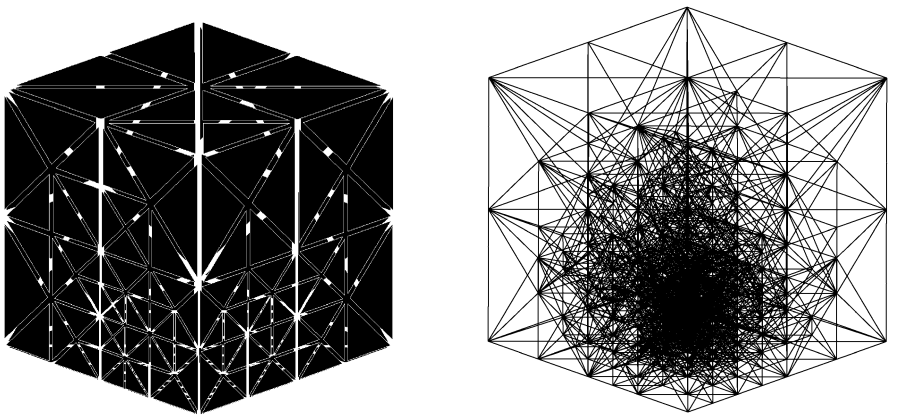

(a) (b)

Fig. 5. Final mesh, 1402 nodes and 7470 tetrahedra: (a) Trace on the cube surface; (b) Complete final mesh.

A tetrahedron shape measure is a continuous function that evaluates the quality of a tetrahedron. It must be invariant under translation, rotation, reflection and uniform scaling of the tetrahedron, maximum for the regular tetrahedron and minimum for a degenerate tetrahedron. There should be no local maximum other than the global maximum for a regular tetrahedron and there should be no local minimum other than the global minimum for a degenerate tetrahedron [3]. Since the shape measure must be invariant under uniform scaling, from now on tetrahedra are considered normalized having the same diameter $\delta(t)$, that is, the length of the longest edge will be the same in all tetrahedra. A degenerate tetrahedron is a tetrahedron whose volume vanishes having diameter greater than zero.

Some measures of mesh quality (or degeneracy) are the following: Whitehead [18] introduced the *relative thickness* of a simplex S: $\rho(S) = \frac{\tilde{r}(S)}{\delta(S)}$, where the *radius* $\tilde{r}(S)$ is defined here as the distance from the centroid of S to its boundary and $\delta(S)$ is the diameter of S.

Stynes [17] introduced $t(S) = \frac{\text{area}(S)}{\delta^2(S)}$, for the bisection method applied to triangles. This ratio can be generalized to higher dimensions such as: $t(S) = \frac{\text{volume}(S)}{\delta^n(S)}$, where n is the dimension of the simplex S. Other authors (see for example [2]) have used $\text{ratio}(S) = \frac{r(S)}{R(S)}$, where $r(S)$ is now the length of the radius of the inscribed sphere and $R(S)$ is the radius of the circumscribed sphere.

For a tetrahedron t and each vertex $P \in t$, Rivara and Levin [14] introduce the measure Φ_P associated with the solid angle Ω_P at P:

$$\Phi_P = \sin^{-1}\left\{\left(1 - \cos^2\alpha_P - \cos^2\beta_P - \cos^2\gamma_P + 2\cos\alpha_P\cos\beta_P\cos\gamma_P\right)^{1/2}\right\},$$

where α_P, β_P, γ_P are the associated corner angles. Then they define $\Phi_t = \min\{\Phi_P\colon\ P \in t\}$. The relation between Φ_P and the solid angle Ω_P at P is the following (see [5,9]):

$$\Omega_P = 2\sin^{-1}\frac{\sin(\Phi_P)}{4\cos(\alpha_P/2)\cos(\beta_P/2)\cos(\gamma_P/2)}.$$

Liu and Joe [4,6] introduced the estimate: $\eta(t) = \frac{3\sqrt[3]{\lambda_1\lambda_2\lambda_3}}{\lambda_1+\lambda_2+\lambda_3}$, where λ_i are the eigenvalues of the matrix $A(R, M) = (MR^{-1}TMR^{-1})$ for matrices M and R associated with a given tetrahedron t and a regular tetrahedron with the same volume as t. They also proved that for any tetrahedron t, $\eta(t) = 12(3v)^{2/3}/\sum_{i=1}^{6} l_i^2$, where v is the volume of t and l_i are the lengths of the edges of t.

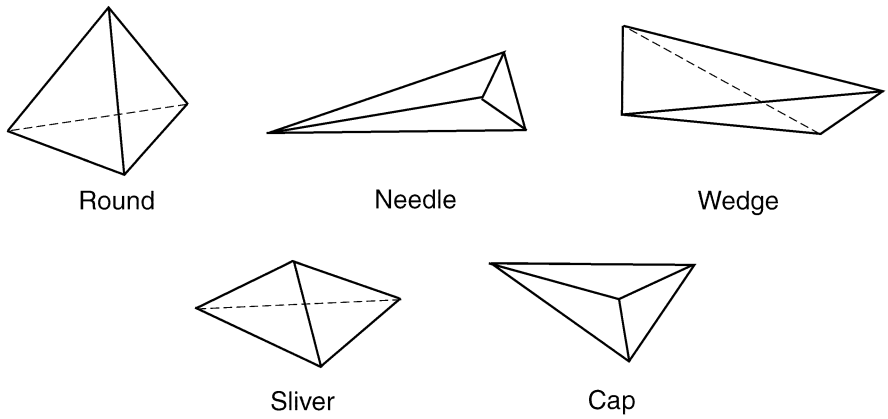

Fig. 6. Shape-based types of tetrahedra.

Table 1
Problems 1–4

P1			P2			P3			P4		
$\eta = 0.8846$			$\eta = 0.8399$			$\eta = 0.2835$			$\eta = 1.0000$		
0.0	0.0	0.0	0.0	0.0	0.0	0.0	0.0	0.0	0.0	0.0	0.0
4.0	2.0	2.0	4.0	0.0	0.0	0.5	0.0	0.0	$2\sqrt{3}$	0.0	0.0
1.0	5.0	0.0	0.0	4.0	0.0	1.0	5.0	2.0	$\sqrt{3}$	3.0	0.0
0.5	0.5	5.0	0.0	0.0	4.0	0.5	0.5	5.0	$\sqrt{3}$	1.0	$2\sqrt{2}$

Fig. 6 shows some common shape-based types of tetrahedra that may occur in refined meshes [2,8]. We give descriptive names to the five different types of three-dimensional simplices: A *round* tetrahedron has no bad angles of any kind. A *needle* or *thin* has one small solid angle. A *wedge-like* element has small but not large dihedrals and no large angles of any kind. A *sliver* has small and large dihedrals, but no large solid angle. A *cap-like* tetrahedron has a large,—nearly flat—solid angle. For the cap tetrahedron, the circumscribed sphere's radius is hence much larger than the longest edge.

We provide here a numerical comparison on the behavior of $\eta_{\min}$, the minimum value of η in the tetrahedra of the mesh, and $\Omega_{\min}$, when the pure longest-edge bisection based refinement, the Liu–Joe partition, and the 8T-LE partition [9] are applied to initial tetrahedra P1, P2, P3, and P4. P1 and P2 are well-shaped tetrahedra; P3 is a poorly shaped tetrahedron and P4 is the regular tetrahedron. In Table 1 these four test problems are listed in terms of the coordinates of their four vertices. They are also studied by Rivara and Levinin [14] and Liu and Joe [6].

Note that the global application of the 8T-LE and Liu–Joe partitions to any initial conforming mesh yield a conforming mesh. However, the longest-edge bisection needs additional refinements in order to get a conforming mesh. This explains the different number of tetrahedra obtained in each column in Table 2.

In these test problems two separate uniform refinements by 8T-LE partition and Liu–Joe partition are applied to each initial tetrahedron, while for the longest-edge bisection we report results for similar number of tetrahedra. Each longest-edge bisection consists in the longest-edge bisection of all the tetrahedra

Table 2
Comparison of Problems 1–4

LE bisection			Liu–Joe partition			8T-LE		
NTET	$\eta_{\min}$	$\Omega_{\min}$	NTET	$\eta_{\min}$	$\Omega_{\min}$	NTET	$\eta_{\min}$	$\Omega_{\min}$
Problem 1								
1	0.885	0.356	1	0.885	0.356	1	0.885	0.356
8	0.682	0.189	8	0.682	0.187	8	0.682	0.187
86	0.479	0.079	64	0.663	0.164	64	0.571	0.142
Problem 2								
1	0.840	0.339	1	0.840	0.339	1	0.840	0.339
8	0.657	0.169	8	0.504	0.091	8	0.504	0.091
102	0.458	0.070	64	0.504	0.091	64	0.504	0.091
Problem 3								
1	0.284	0.047	1	0.284	0.047	1	0.284	0.047
8	0.181	0.024	8	0.181	0.024	8	0.181	0.024
192	0.165	0.014	64	0.170	0.022	64	0.163	0.014
Problem 4								
1	1.00	0.551	1	1.00	0.551	1	1.00	0.551
8	0.546	0.132	8	0.546	0.132	8	0.546	0.132
306	0.458	0.070	64	0.429	0.070	64	0.429	0.070

of the previous level, followed by the longest-edge bisection of the non-conforming tetrahedra until a conforming mesh is obtained.

The left part of Table 2 shows the results reproduced based on the longest edge bisection [14]. The middle part of the Table 2 is for the Liu–Joe partition [6]. Note that the results using 8T-LE partition in the right column are comparable to those obtained by the longest edge bisection of Rivara and Levin [14] and by the Liu and Joe partition [6].

Although the comparison illustrates that the numerical results are similar among the reported partitions, in next sections we will give a more adequate insight on the non-degeneracy property of the 8T-LE partition. We proceed by studying meshes obtained from many different shaped tetrahedra based on previous sensitivity tests of the shape measures, having in the finest mesh more than two millions tetrahedra. Our goal is to obtain an experimental coefficient of non-degeneracy for the 8-tetrahedra longest-edge partition and to compare it with the theoretical value obtained by Liu and Joe [4]. Although we do not provide examples with a complex initial mesh taken from a real application, the wide variety of shapes in the studied tetrahedra allows us to conjecture that the non-degeneracy coefficient will be very close to the empirical non-degeneracy coefficient given in this paper.

5. Sensitivity tests

The aim of this section is to design a set of geometric transformations, called here sensitivity tests, to be applied to a regular tetrahedron. Several sensitivity tests have been used together with the shape measures for the comparison and evaluation of tetrahedron quality measures [3,8]. We study the behavior of

some of the previously mentioned shape measures beginning with a regular tetrahedron with coordinates $(0, 0, 0)$ for vertex 1, $(2\sqrt{3}, 0, 0)$ for vertex 2, $(\sqrt{3}, 3, 0)$ for vertex 3, and finally $\sqrt{3}, 1, 2\sqrt{2})$ for the apex. The sensitivity tests are as follows:

(1) The apex is moved in small increments along the vertical axis and approaching the supporting face, see Fig. 7(a). This process is carried out defining the third coordinate of the apex in this way: $\frac{2\sqrt{2}}{i}$, where $i = 1, \ldots, 20$. Note that for locations of the apex close to the base, the test simulates a *cap* element.
(2) The apex is moved in small increments along the edge joining vertices 1 and 4 to vertex 1, see Fig. 7(b). That is, if vertex 4 is D, and $\vec{v}$ is the vector between vertices 4 and 1, then the coordinates of the respective new apex D_i are given by $D_i = D - \frac{i-1}{20}\vec{v}$. In this test, for locations of the apex near the other vertex, degenerate elements of the type *wedge* are obtained.
(3) The apex is allowed to trace in small increments a quarter-arc defined using the height of the tetrahedron as the radius, see Fig. 7(c). In this test, for locations of the apex near the base, degenerate elements of the type *sliver* are obtained.
(4) The apex is moved away from the supporting face defining the third coordinate of the apex in this way: $2\sqrt{2}i$, where $i = 1, \ldots, 20$. Note that in Fig. 7(d) only normalized tetrahedra, having the same diameter, have been drawn. Degenerate elements of the type *needle* are obtained.

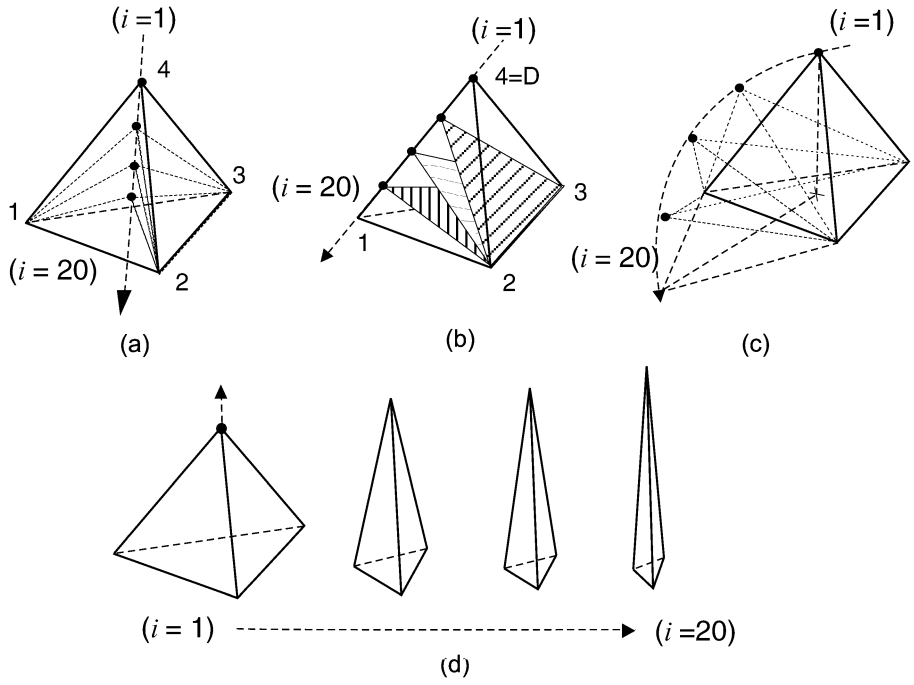

Fig. 7. Sensitivity tests: (a) the apex is moved along the vertical axis, (b) the apex is moved along one edge, (c) the apex is moved along a quarter-arc, (d) the apex is moved along the vertical axis away from the supporting face.

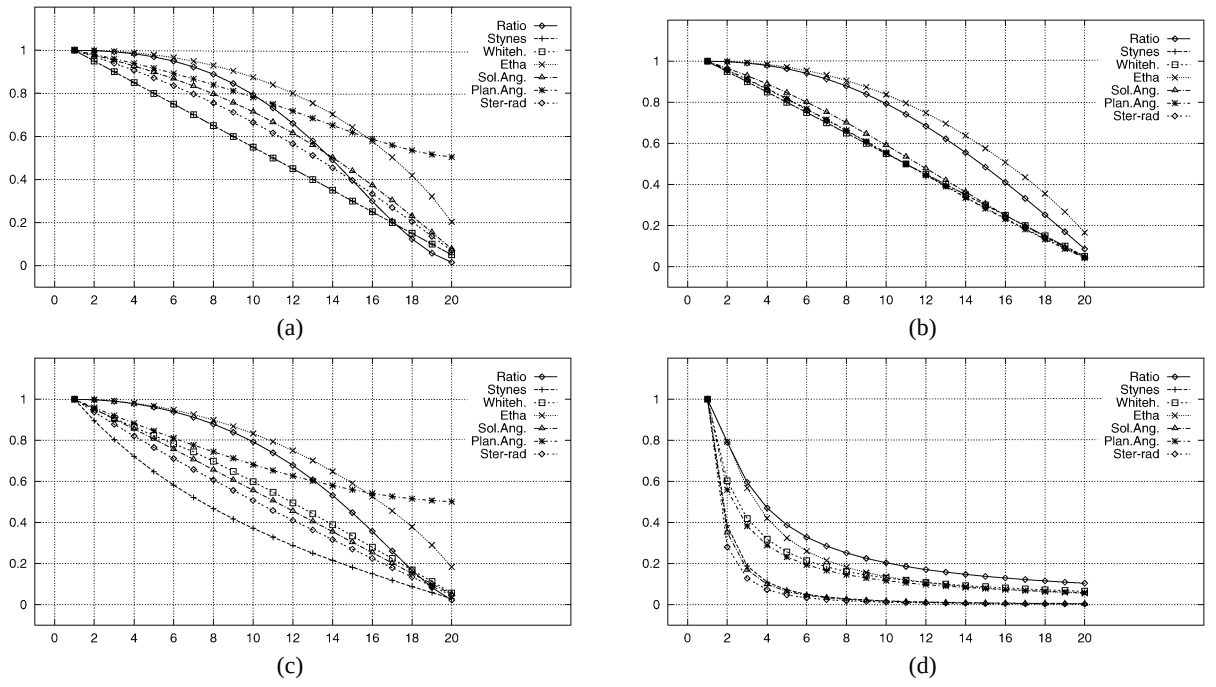

Fig. 8. Comparison of shape measures considering Tests 1–4. Ratio $= \frac{r(S)}{R(S)}$, Stynes $= \frac{\text{volume}(S)}{\delta^3(S)}$, Whiteh. $= \frac{\tilde{r}(S)}{\delta(S)}$, Etha $= \eta(S)$, Sol.Ang. $= \Omega_{\min}$, Plan.Ang. $=$ min planar angle, Ster-rad. $= \Phi_{\min}$: (a) Test 1: Apex moves to the supporting face; (b) Test 2: Apex moves along one edge; (c) Test 3: Apex moves a quarter-arc; (d) Test 4: Apex moves away from the supporting face.

Note that for ease of comparison, the shape measures have been scaled to the interval $[0, 1]$, with 1 being for the regular tetrahedron and 0 for a degenerate tetrahedron.

Fig. 8 shows the evolution of different shape measures for the tetrahedra obtained during the four tests explained before. From the results reported Fig. 8(a) and (c), it can be noted that the minimum planar angle is not a good shape measure for tetrahedra since it can be greater than zero for planar tetrahedra. The remaining shape measures show a similar behavior in the tests. This is in complete agreement with other previous works [5,8].

6. Empirical study of the non-degeneracy of the 8T-LE partition

Rivara and Levin in [14] reported an empirical study of the reduction of the solid angle size due to repeated subdivision by the pure longest-edge bisection of tetrahedra. Their results allowed to conjecture that the shape function associated to the minimum angle $\Phi_{\min}(k)$, where k is the bisection iteration, converges asymptotically to a fixed value.

Let t be an initial tetrahedron in which the 8T-LE partition is applied. Thus, from the initial mesh $\tau^1 = \{t = t_1^1\}$, mesh $\tau^2 = \{t_i^2\}$ is obtained. The successive application of the 8T-LE partition to any tetrahedron and its successors yields an infinite sequence of tetrahedral meshes $\tau^1, \tau^2, \tau^3, \ldots$.

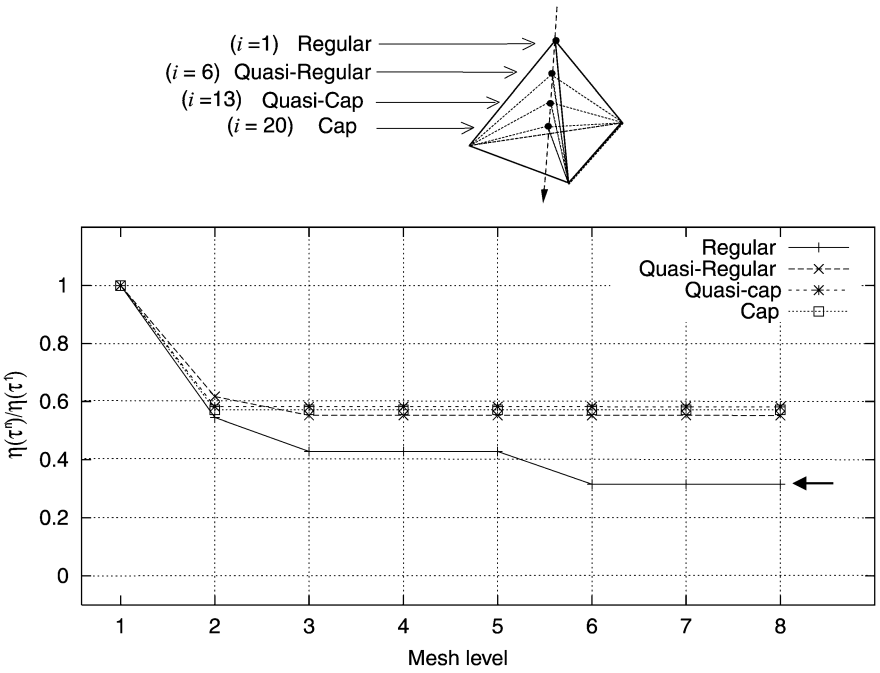

Fig. 9. Experiment 1: Four initial tetrahedra considered and evolution of degeneracy constant.

Table 3
Shape measures (η), mesh τ^8 with 2 097 152 elements for 4 different initial tetrahedra t_1^1

t_1^1	$\eta(t_1^1)$	Normalized η	$\min\{\eta(t_i^8)\}$	$c_8 = \frac{\eta(\tau^8)}{\eta(\tau^1)}$
Regular	1.000	1.000	0.31553	0.31553
Quasi-regular	0.929	1.000	0.51294	0.55199
Quasi-cap	0.643	1.000	0.37439	0.58202
Cap	0.203	1.000	0.11622	0.57158

We give here experimental evidence showing that for a standard shape measure (η), the non-degeneracy convergence to a fixed positive value is guaranteed, that is, for any tetrahedron t_i^n in τ^n, $n \geqslant 1$,

$$\eta\left(t_i^n\right) \geqslant c\eta(t) \tag{2}$$

where c is constant and independent of i and n. With this aim, we perform seven 8T-LE global refinements beginning with an initial mesh $\tau^1 = \{t_1^1\}$. This initial mesh contains one different initial tetrahedron in each case. The refinement process ends with the mesh level τ^8 containing $8^7 = 2\,097\,152$ elements.

As a quality measure of τ^n we define $\eta(\tau^n) = \min\{\eta(t_i^n)\}$ for all $t_i^n \in \tau^n$. Then the value

$$c_n = \frac{\eta(\tau^n)}{\eta(\tau^1)} \tag{3}$$

is calculated. This value is taken as an estimation of c in Eq. (2).

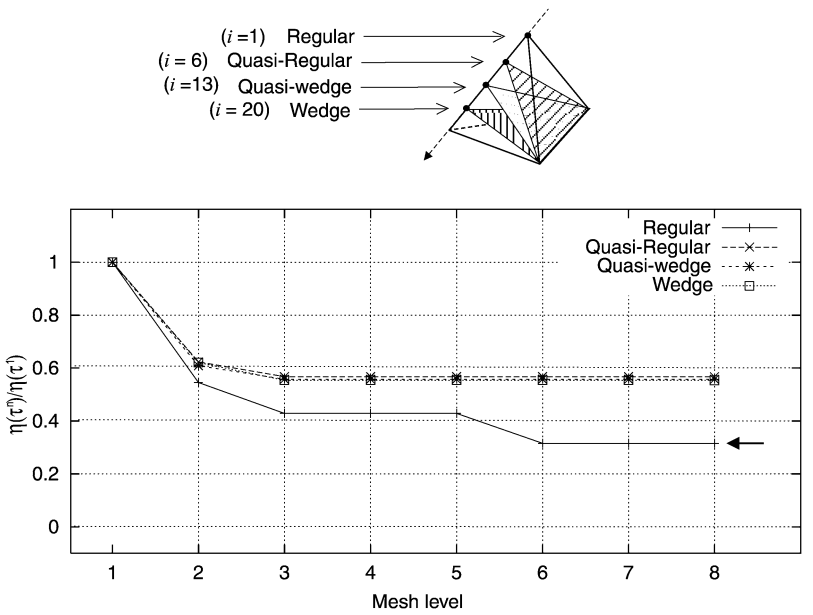

Fig. 10. Experiment 2: Initial tetrahedra and evolution of degeneracy constant.

Table 4
Shape measures (η), mesh τ^8 with 2 097 152 elements for four different initial tetrahedra t_1^1

t_1^1	$\eta(t_1^1)$	Normalized η	$\min\{\eta(t_i^8)\}$	$c_8 = \frac{\eta(\tau^8)}{\eta(\tau^1)}$
Regular	1.000	1.000	0.31553	0.31553
Quasi-regular	0.906	1.000	0.51415	0.56728
Quasi-wedge	0.576	1.000	0.32116	0.55779
Wedge	0.166	1.000	0.09191	0.55390

6.1. First experiment

This experiment considers four different initial tetrahedra chosen from the first sensitivity test. We perform seven 8T-LE global refinements in each case. The finest mesh τ^8 contains $8^7 = 2\,097\,152$ elements. Table 3 summarizes the results and Fig. 9 presents the evolution of the values of $c_n = \frac{\eta(\tau^n)}{\eta(\tau^1)}$.

It is worth noting that the most unfavorable case for the degeneracy constant c_8 corresponds to the regular tetrahedron as initial mesh ($c_8 = 0.315$). The other tetrahedra (for values $i = 6, 13, 20$) show similar behavior ($c_8 > 0.55$).

6.2. Second experiment

This experiment considers four different initial tetrahedra chosen from the second sensitivity test and proceeds as the first experiment. Table 4 summarizes the results and Fig. 10 gives the evolution of $c_n = \frac{\eta(\tau^n)}{\eta(\tau^1)}$. Note that the results are analogous to those in experiment 1.

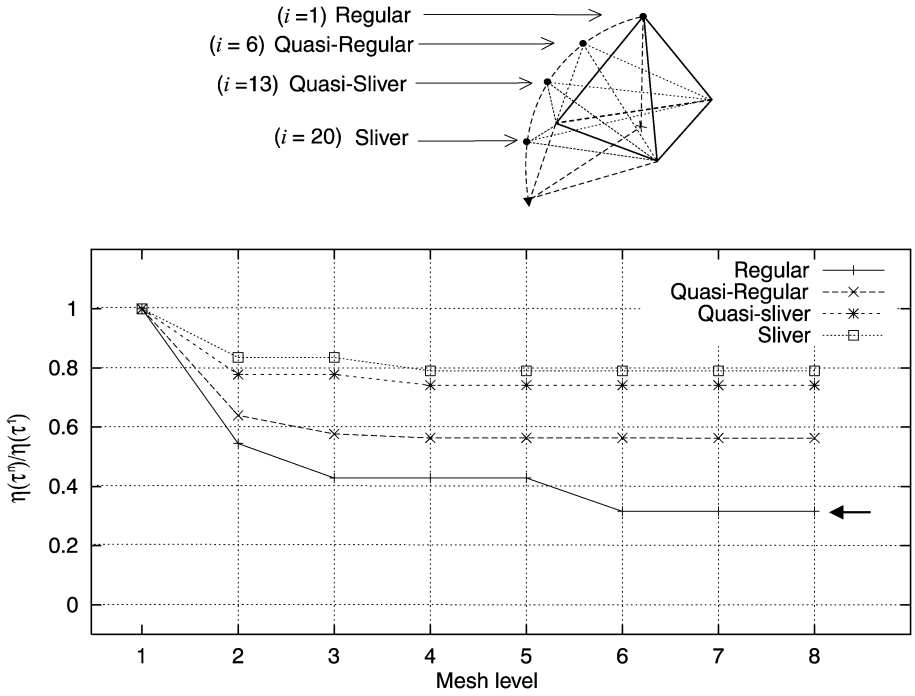

Fig. 11. Experiment 3: Initial tetrahedra and evolution of degeneracy constant.

Table 5
Shape measures (η), mesh τ^8 with 2 097 152 elements for four different initial tetrahedra t_1^1

t_1^1	$\eta(t_1^1)$	Normalized η	$\min\{\eta(t_i^8)\}$	$c_8 = \frac{\eta(\tau^8)}{\eta(\tau^1)}$
Regular	1.000	1.000	0.31553	0.31553
Quasi-regular	0.949	1.000	0.53439	0.56335
Quasi-sliver	0.702	1.000	0.52018	0.74132
Sliver	0.183	1.000	0.14484	0.79030

6.3. Third experiment

This experiment considers four different initial tetrahedra chosen from the third sensitivity test and proceeds as before. Table 5 summarizes the results and Fig. 11 gives the values of $c_n = \frac{\eta(\tau^n)}{\eta(\tau^1)}$. In this experiment we observe an increasing improvement for c_8 as the initial tetrahedron degenerates. The highest value of c_8 is for the sliver tetrahedron ($i = 20$).

6.4. Fourth experiment

This experiment considers four different initial tetrahedra chosen from the fourth sensitivity test and proceeds as before. Table 6 summarizes the results and Fig. 12 gives again the values of $c_n = \frac{\eta(\tau^n)}{\eta(\tau^1)}$. The most favorable cases in this experiment are for the quasi-needle and needle tetrahedra.

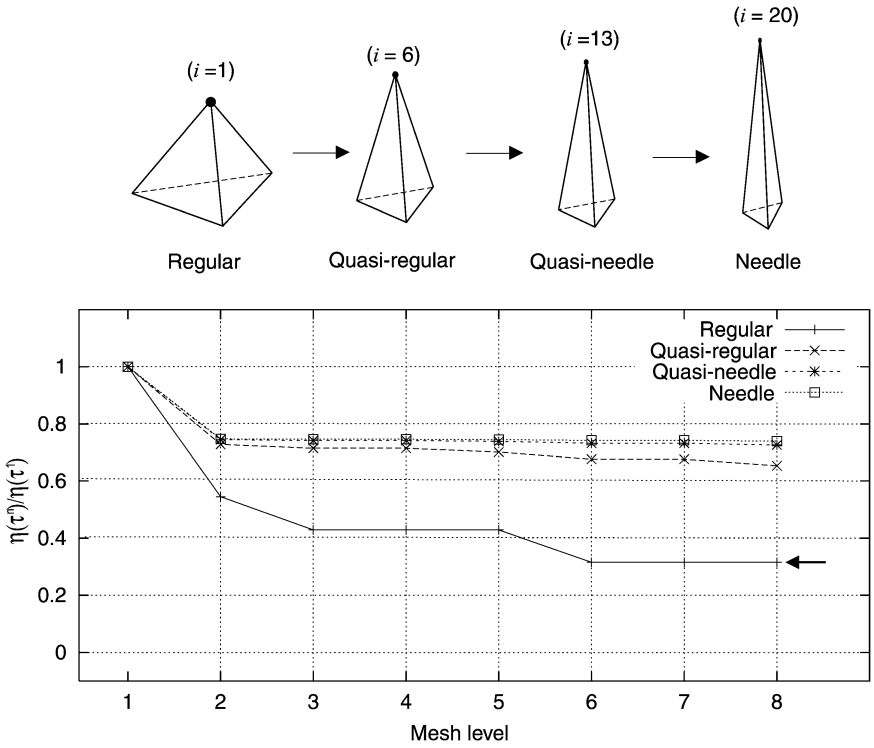

Fig. 12. Experiment 4: Initial tetrahedra and evolution of degeneracy constant.

Table 6
Shape measures (η), mesh τ^8 with 2 097 152 elements for four different initial tetrahedra t_1^1

t_1^1	$\eta(t_1^1)$	Normalized η	$\min\{\eta(t_i^8)\}$	$c_8 = \frac{\eta(\tau^8)}{\eta(\tau^1)}$
Regular	1.000	1.000	0.31553	0.31553
Quasi-regular	0.261	1.000	0.17030	0.65329
Quasi-needle	0.097	1.000	0.07043	0.72608
Needle	0.055	1.000	0.04067	0.73958

It should be noted that the most unfavorable case in all the experiments corresponds to the regular tetrahedron as initial mesh. This fact is in accordance with the behavior of the 4T-LE partition in two dimensions, in which the lowest bound of degeneracy for the angles is reached ($\alpha_n = \frac{1}{2}\alpha_0$) for the equilateral triangle. On the other hand, in the last two experiments, the best case for the degeneracy constant corresponds to the worst initial tetrahedron, sliver tetrahedron in experiment 3 and needle tetrahedron in experiment 4. From Figs. 9–12 and Tables 1–4 we deduce that the estimated value for the non-degeneracy constant is $c = 0.31553$.

7. Conclusions

We have reported here numerical evidence on the non-degeneracy property of the 8T-LE partition: For the standard shape measure η, the non-degeneracy convergence to a fixed positive value is guaranteed. The 8T-LE partition is applied to an initial tetrahedron t and its successors, so that a sequence of tetrahedral meshes $\tau^1, \tau^2, \tau^3, \ldots, \tau^8$ is obtained. For any tetrahedron t_i^n, in τ^n, $1 \leqslant n \leqslant 8$, $\eta(t_i^n) \geqslant c\eta(t)$ and c is a constant ($c = 0.31553$) independent of i and n. Although we do not provide any formal proof of the non-degeneracy property of the 8T-LE partition, this result helps to state the conjecture that this partition verifies the non-degeneracy property, and also to discard the idea that for the three-dimensional case it could be proved that $\eta(t_i^n) \geqslant \frac{1}{3}\eta(t)$.

References

[1] I. Babuška, A.K. Aziz, On the angle condition in the finite element method, SIAM J. Numer. Anal. 13 (2) (1976) 214–226.
[2] M. Bern, D. Eppstein, Mesh generation and optimal triangulation, in: D.-Z. Du, F.K. Hwang (Eds.), Computing in Euclidean Geometry, second ed., World Scientific, Singapore, 1995, pp. 47–123.
[3] J. Dompierre, P. Labbé, F. Guibault, R. Camarero, Benchmarks for 3D unstructured tetrahedral mesh optimization, in: 7th Int. Mes. Roundt., Sandia Report SAND 98-2250, 1998, pp. 459–478.
[4] A. Liu, B. Joe, On the shape of tetrahedra from bisection, Math. Comp. 63 (1994) 141–154.
[5] A. Liu, B. Joe, Relationship between tetrahedron shape measures, BIT 34 (1994) 268–287.
[6] A. Liu, B. Joe, Quality local refinement of tetrahedral meshes based on bisection, SIAM J. Sci. Statist. Comput. 16 (1995) 1269–1291.
[7] W.F. Mitchell, A comparison of adaptive refinement technique for elliptic problems, ACM Trans. Math. Software 15 (4) (1989) 326–347.
[8] V.N. Parthasarathy, C.M. Graichen, A.F. Hathaway, A comparison of tetrahedron quality meshes, Finite Elem. Anal. Des. 15 (1993) 225–261.
[9] A. Plaza, G.F. Carey, Refinement of simplicial grids based on the skeleton, Appl. Numer. Math. 32 (2) (2000) 195–218.
[10] A. Plaza, M.A. Padrón, G.F. Carey, A 3D refinement/derefinement combination to solve evolution problems, Appl. Numer. Math. 32 (4) (2000) 285–302.
[11] A. Plaza, M.C. Rivara, Asymptotic behavior of the average adjacencies for skeleton-regular triangular and tetrahedral partitions, J. Comput. Appl. Math. 140 (1–2) (2002) 673–693.
[12] M.C. Rivara, Mesh refinement based on the generalized bisection of simplices, SIAM J. Numer. Anal. 2 (1984) 604–613.
[13] M.C. Rivara, Selective refinement/derefinement algorithms for sequences of nested triangulations, Internat. J. Numer. Methods Engrg. 28 (1989) 2889–2906.
[14] M.C. Rivara, C. Levin, A 3-d refinement algorithm suitable for adaptive and multi-grid techniques, Comm. Appl. Numer. Methods 8 (1992) 281–290.
[15] M.C. Rivara, G. Iribarren, The 4-triangles longest-side partition of triangles and linear refinement algorithms, Math. Comp. 65 (1996) 1485–1502.
[16] I.G. Rosenberg, F. Stenger, A lower bound on the angles of triangles constructed by bisecting the longest side, Math. Comp. 29 (130) (1975) 390–395.
[17] M. Stynes, On faster convergence of the bisection method for all triangles, Math. Comp. 35 (152) (1980) 1195–1201.
[18] J.H.C. Whitehead, On C^1-complexes, Ann. of Math. 41 (1940) 809–824.
[19] A. Ženíšek, The maximum angle condition in the finite element method for monotone problems with applications in magnetostatics, Numer. Math. 71 (3) (1995) 399–417.